3

Free Vibration Analysis of Curved Sandwich Beams: A Dynamic Finite Element

Seyed M. Hashemi and Ernest J. Adique
Ryerson University
Canada

1. Introduction

Applications of sandwich construction and composites continue to expand. They are used in a number of industries such as the aerospace, automotive, marine and even sports equipment. Sandwich construction offers designers high strength to weight ratios, as well as good buckling resistance, formability to complex shapes and easy reparability, which are of extremely high importance in aerospace applications. Due to their many advantages over traditional aerospace materials, the analysis of sandwich beams has been investigated by a large number of authors for more than four decades. Sandwich construction can also offer energy and vibration damping when a visco-elastic core layer is used. However, such non-conservative systems are not the focus of the present study.

The most common sandwich structure is composed of two thin face sheets with a thicker lightweight, low-stiffness core. Common materials used for the face layers are metals and composite while the core is often made of foam or a honeycomb structure made of metal. It is very important that the core, although weaker than the face layers, be strong enough to resist crushing. The current trend in the aerospace industry of using composites and sandwich material, to lighten aircraft in an attempt to make them more fuel efficient, has led to further recent researches on development of reliable methods to predict the vibration behaviour of sandwich structures.

In the late 1960s, pioneering works in the field of vibration analysis of viscously damped sandwich beams (Di Taranto, 1965, and Mead and Marcus, 1968) used classical methods to solve the governing differential equations of motion, leading to the natural frequencies and mode shapes of the system. Ahmed (1971) applied the finite element method (FEM) to a curved sandwich beam with an elastic core and performed a comparative study of several different formulations in order to compare their performances in determining the natural frequencies and mode shapes for various different beam configurations. Interest in the vibration behaviour of sandwich beams has seen resurgence in the past decade with the availability of more powerful computing systems. This has allowed for more complex finite element models to be developed. Sainsbury and Zhang (1999), Baber et al. (1998), and Fasana and Marchesiello (2001) are just some among many researchers who investigated FEM application in the analysis of visco-elastically damped sandwich beams. The Dynamic Stiffness Method (DSM), which employs symbolic computation to combine all the governing differential equations of motion into a single ordinary differential equation, has also been well established. Banerjee and his co-workers (1995-2007) and Howson and Zare (2005) have published numerous papers on DSM illustrating its successful application to numerous homogeneous and sandwich/composite beam configurations, with a number of papers focusing on elastic-core sandwich beams. It is worth noting that in all the above-mentioned sandwich element models, the beam motion is assumed to exhibit coupled bending-axial motion only, with no torsional or out-of-plane motion. Also, the layers are assumed to be perfectly and rigidly joined together and the interaction of the different materials at the interfaces is ignored. Although it is known that bonding such very much different materials will cause stress at the interfaces, the study of their interactions and behaviour at the bonding site is another research topic altogether and is beyond the scope of the present Chapter.

Another important factor that largely affects the results of the sandwich beam analysis is the assumed vibration behaviour of the layers. The simplest sandwich beam model utilizes Euler-Bernoulli theory for the face layers and only allows the core to deform only in shear. This assumption has been widely used in several DSM and FEM studies such as those by Banerjee (2003), Ahmed (1971,1972), Mead and Markus (1968), Fasana and Marchesiello (2001), Baber et al. (1998), and in earlier papers by the authors; see e.g., Adique & Hashemi (2007), and Hashemi & Adique (2009). In more recent publications, Banerjee derived two new DSM models which exploit more complex displacement fields. In the first and simpler of the two (Banerjee & Sobey, 2005), the core bending is governed by Timoshenko beam theory, whereas the face plates are modeled as Rayleigh beams. To the authors' best knowledge, the most comprehensive sandwich beam theory was developed and used by Banerjee et al. (2007), where all three layers are modeled as Timoshenko beams. However, increasing the complexity of the model also significantly increases the amount of numerical and symbolic computation in order to achieve the complete formulation.

Classical FEM method has a proven track record and is the most commonly used method for structural analysis. It is a systematic approach, leading to element stiffness and mass matrices, easily adaptable to a wide range of problems. The polynomial shape functions are used to approximate the displacement fields, resulting in a linear eigenproblem, whose solutions are the natural frequencies of the system. Most commercial FEM-based structural analysis software also offer multi-layered elements that can be used to model layered composite materials and sandwich construction (e.g., ANSYS® and MSC NASTRAN/PATRAN®). As a numerical formulation, however, the versatility of the FEM theory comes with a drawback; the accuracy of its results depends on the number of elements used in the model. This is the most evident when FEM is used to evaluate system behaviour at higher frequencies, where a large number of elements are needed to achieve accurate results.

Dynamic Stiffness Matrix (DSM) method, on the other hand, provides an analytical solution to the free vibration problem, achieved by combining the coupled governing differential equations of motion of the system into a single higher order ordinary differential equation. Enforcing the boundary conditions then leads to the system's DSM and the most general closed form solution is then sought. The DSM formulation results in a non-linear eigenvalue problem and the bi-section method, combined with the root counting algorithm developed by Wittrick & Williams (1971), is then used as a solution technique. DSM provides exact results (i.e., closed form solution) for any of the natural frequencies of the beam, or beam-structure, with the use of a single continuous element characterized by an infinite number of degrees of freedom. However, the DSM methods is limited to special cases, for which the closed form solution of the governing differential equation is known; e.g., systems with constant geometric and material properties and only a certain number of boundary conditions.

The Dynamic Finite Element (DFE) method is a hybrid formulation that blends the well-established classical FEM with the DSM theory in order to achieve a model that possesses all the best traits of both methods, while trying to minimize the effects of their limitations; i.e., to fuse the adaptability of classical FEM with the accuracy of DSM. Therefore, the approximation space is defined using frequency dependent trigonometric basis functions to obtain the appropriate interpolation functions with constant parameters over the length of the element. DFE theory was first developed by Hashemi (1998), and its application has ever since been extended by him and his coworkers to the vibration analysis of intact (Hashemi et al.,1999, and Hashemi & Richard, 2000a,b) and defective homogeneous (Hashemi et al., 2008), sandwich (Adique & Hashemi, 2007-2009, and Hashemi & Adique, 2009, 2010) and laminated composite beam configurations (Hashemi & Borneman, 2005, 2004, and Hashemi & Roach, 2008a,b) exhibiting diverse geometric and material couplings. DFE follows a very similar procedure as FEM by first applying the weighted residual method to the differential equations of motion. Next, the element stiffness matrices are derived by discretizing the integral form of the equations of motion. For FEM, the polynomial interpolation functions are used to express the field variables, which in turn are introduced into the integral form of the equations of motion and the integrations are carried out and evaluated in order to obtain the element matrices. At this point, DFE applies an additional set of integration by parts to the element equations, introduces the Dynamic Trigonometric Shape Functions (DTSFs), and then carries out the integrations to form the element matrices. In the case of a three-layered sandwich beam, the closed form solutions to the uncoupled parts of the equations of motion are used as the basis functions of the approximation space to develop the DTSFs. The assembly of the global stiffness matrix from the element matrices follows the same procedure for FEM, DSM and DFE methods. Like DSM, the DFE results in a non-linear eigenvalue problem, however, unlike DSM, it is not limited to uniform/stepped geometry and can be readily extended to beam configurations with variable material and geometric parameters; see e.g., Hashemi (1998).

In the this Chapter, we derive a DFE formulation for the free vibration analysis of curved sandwich beams and test it against FEM and DSM to show that DFE is another viable tool for structural vibration analysis. The face layers are assumed to behave according to Euler-Bernoulli theory and the core deforms in shear only, as was also studied by Ahmed (1971,1972). The authors have previously developed DFE models for two straight, 3-layered, sandwich beam configurations; a symmetric sandwich beam, where the face layers are assumed to follow Euler-Bernoulli theory and core is allowed to deform in shear only (Adique & Hashemi, 2007, and Hashemi & Adique, 2009), and a more general non-symmetric model, where the core layer of the beam behaves according to Timoshenko theory while the faces adhere to Rayleigh beam theory (Adique & Hashemi, 2008, 2009). The latter model not only can analyze sandwich beams, where all three layers possess widely different material and geometric properties, but also it has shown to be a quasi-exact formulation (Hashemi & Adique, 2010) when the core is made of a soft material.

2. Mathematical model

Figure 1 below shows the notation and corresponding coordinate system used for a symmetrical curved three-layered sandwich beam with a length of S and radius R at the mid-plane of the beam. The thicknesses of the inner and outer face layers are t while the thickness of the core is represented by t_c. In the coordinate system shown, the z-axis is the normal co-ordinate measured from the centre of each layer and the y-axis is the circumferential coordinate and coincides with the centreline of the beam. The beam only deflects in the y-z plane. The top and bottom faces, in this case, are modelled as Euler-Bernoulli beams, while the core is assumed to have only shear rigidity (e.g., the stresses in the core in the longitudinal direction are zero). The centreline displacements of layers 1 and 3 are v_1 and v_2, respectively. The main focus of the model is flexural vibration, w, and is common among all three layers, which leads to the assumption $v_1 = -v_2 = -v$.

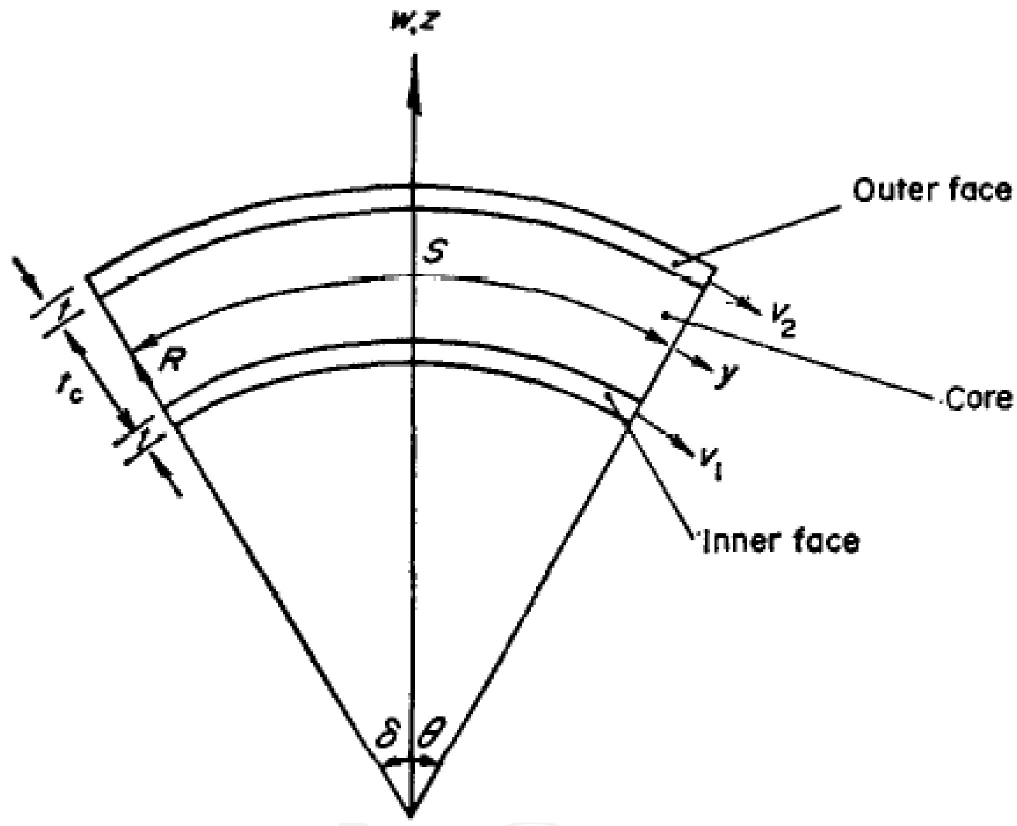

Fig. 1. Coordinate system and notation for curved symmetric three-layered sandwich beams

For the beam model developed, the following assumptions made (Ahmed, 1971):

- All displacements and strains are so small that the theory of linear elasticity still applies.
- The face materials are homogeneous and elastic, while the core material is assumed to be homogeneous, orthotropic and rigid in the z-direction.
- The transverse displacement w does not vary throughout the thickness of the beam.
- The shear within the faces is negligible.
- The bending strain within the core is negligible.
- There is no slippage or delamination between the layers during deformation.

Using the model and assumptions described above, Ahmed (1971) used the principle of minimum potential energy to obtain the differential equations of motion and corresponding boundary conditions. For free vibration analysis, the assumption of simple harmonic motion is used, leading to the following form of the differential equations of motion for a curved symmetrical sandwich beam (Ahmed, 1971):

$$\frac{\partial^2 v}{\partial y^2} + \frac{1}{\alpha^2}(\omega^2 Q_1 - 4\beta^2)v - \frac{2h\beta^2}{\alpha^2}\frac{\partial w}{\partial y} = 0, \tag{1}$$

$$\frac{\partial^4 w}{\partial y^4} - \frac{h^2\beta^2}{\gamma^2}\frac{\partial^2 w}{\partial y^2} + \frac{1}{\gamma^2}(\frac{\alpha^2}{R^2} - \omega^2 Q_2)w - \frac{2h\beta^2}{\gamma^2}\frac{\partial v}{\partial y} = 0, \tag{2}$$

where

$$\begin{aligned} &\alpha^2 = 2Et, \quad \beta^2 = (1/t_c + t_c/4R^2)G_c, \quad \gamma^2 = Et^3/6, \\ &h = t + t_c, \quad Q_1 = 2t\rho_f + t_c\rho_c/3, \quad Q_2 = 2t\rho_f + t_c\rho_c. \end{aligned} \tag{3}$$

In the equations above, $v(y)$ and $w(y)$ are the amplitudes of the sinusoidally varying circumferential and radial displacements, respectively. E is the Young's modulus of the face layers, G_c is the shear modulus of the core layer, and ρ and ρ_c are the mass densities of the face and core materials, respectively. The appropriate boundary conditions are imposed at y=0 and y=S. For example, for

- clamped at $y = 0$ and $y = S$; $v = w = \partial w/\partial y = 0$.
- simply supported at $y = 0$ and $y = S$; $\partial v/\partial y = w = \partial^2 w/\partial y^2 = 0$.
- cantilever configuration; at $y = 0$: $v=w=\partial w/\partial y=0$; and at $y=S$: $\partial v/\partial y=\partial^2 w/\partial y^2=0$ and a resultant force term of $[2\gamma^2\partial^3 w/\partial y^3 + 2\beta^2 h(2v + h\partial w/\partial y)] = 0$, …

For harmonic oscillation, the weak form of the governing equations (1) and (2) are obtained by applying a Galerkin-type integral formulation, based on the weighted-residual method. The method involves the use of integration by parts on different elements of the governing differential equations and then the discretization of the beam length into a number of two-node beam elements (Figure 2).

Fig. 2. Domain discretized by N number of 2-noded elements

Applying the appropriate number of integration by parts to the governing equations and discretization lead to the following form (in the equations below, primes denote integration with respect to y):

$$W_v^k = \int_0^l \delta v' \alpha^2 v' dy - \int_0^l \delta v(\omega^2 Q_1 - 4\beta^2) v dy + \int_0^l \delta v 2h\beta^2 w' dy \tag{4}$$

$$W_w^k = \int_0^l \delta w'' \gamma^2 w'' dy + \int_0^l \delta w' h^2 \beta^2 w' dy + \int_0^l \delta w(\alpha^2/R^2 - \omega^2 Q_2) w dy + \int_0^l \delta w' 2h\beta^2 v dy \tag{5}$$

All of the resulting global boundary terms produced by integration by parts before discretization in the equations above are equal to zero. The above equations are known as the *element* Galerkin-type weak form associated to the discretized equations (4) and (5) and also satisfy the principle of virtual work:

$$W = W_{INT} - W_{EXT} = (W_v + W_w) - W_{EXT} = 0 \tag{6}$$

For the free vibration analysis, $W_{EXT} = 0$, and

$$W_{INT} = \sum_{k=1}^{\text{Number of Elements}} W^k;\ \text{where}\ W^k = W_v^k + W_w^k \tag{7}$$

In the equations above, δv and δw are the test- or weighting -functions, both defined in the same approximation spaces as v and w, respectively. Each element is defined by nodes j and $j+1$ with the corresponding co-ordinates ($l=x_{j+1}-x_j$). The admissibility condition for finite element approximation is controlled by the undiscretized forms of equations (4) and (5).

3. Finite elements method (FEM) derivations

Two different FEM models were derived for the curved beam model. The first one has three degrees of freedom (DOFs) per node and uses a linear approximation for the axial displacement and a Hermite type polynomial approximation for the bending displacement.

$$v(y) = < N(y)_v > \{v_j \ \ v_{j+1}\} = N_{1v}(y)v_j + N_{2v}(y)v_{j+1} \tag{8}$$

$$w(y) = < N(y)_w > \{w_j \ w'_j \ w_{j+1} \ w'_{j+1}\} = N_{1w}(y)w_j + N_{2w}(y)w'_j + N_{3w}(y)w_{j+1} + N_{4w}(y)w'_{j+1} \tag{9}$$

In the equations above, v_j, v_{j+1}, w_j and w_{j+1} are the nodal values at j and $j+1$ corresponding to the circumferential and radial displacements, respectively (these can be likened to the axial and flexural displacements for a straight beam). w_j' and w'_{j+1} represent the nodal values of the rate of change of the radial displacements with respect to x (which can be likened to the bending slope for a straight beam). The same approximations were also used for δv and δw, respectively. The first FEM formulation is achieved when the nodal approximations expressed by equations (8) and (9) are applied to simplify equations (4) and (5). Similar approximations are also used for the corresponding test functions, δv and δw, and the integrations are performed to arrive at the classical linear (in ω^2) eigenvalue problem as functions of constant mass and stiffness matrices, which can be solved using programs such as Matlab®.

In the second FEM model the number of DOFs per node is increased to four and Hermite-type polynomial approximations are used for both the axial and bending displacements.

$$v(y) = < N(y)_v > \{v_j \ v'_j \ v_{j+1} \ v'_{j+1}\} = N_{1v}(y)v_j + N_{2v}(y)v'_{j+1} + N_{3v}(y)v_{j+1} + N_{4v}(y)v'_{j+1} \tag{10}$$

$$w(y) = < N(y)_w > \{w_j \ w'_j \ w_{j+1} \ w'_{j+1}\} = N_{1w}(y)w_j + N_{2w}(y)w'_j + N_{3w}(y)w_{j+1} + N_{4w}(y)w'_{j+1} \tag{11}$$

In the equations above, v_j, v_{j+1}, w_j and w_{j+1} are the nodal values at j and $j+1$ corresponding to the circumferential and radial displacements, respectively. v_j', v'_{j+1}, w_j' and w'_{j+1} are the nodal values at j and $j+1$ for the rate of change with respect to y for the circumferential and radial displacements, respectively. The same approximations are also used for δv and δw. The second FEM formulation applies equations (10) and (11) to simplify equations (4) and (5) to produce the linear (in ω^2) eigenvalue problem as a function of constant mass and stiffness matrices, which can again be solved using programs such as Matlab®. For the current research, both FEM models were programmed using Matlab®.

4. Dynamic finite element (DFE) formulation

In order to obtain the DFE formulation, an additional set of integration by parts are applied to the element equations (4) and (5) leading to:

$$W_V^k = \underbrace{-\int_0^l (\delta v''\alpha^2 + \delta v\omega^2 Q_1)vdy}_{(*)} + \underbrace{\int_0^l \delta v(4\beta^2)vdy + [\delta v'\alpha^2 v]_0^l}_{[k]_V^k \text{ Uncoupled}} + \underbrace{\int_0^l (\delta v 2h\beta^2)w'dy}_{[k_{VW}]_{2\times4} \text{ Coupling}} \tag{12}$$

$$\begin{aligned} W_W^k = & \underbrace{\int_0^l (\delta w''''\gamma^2 - \delta w''h^2\beta^2 + \delta w(\alpha^2/R^2 - \omega^2 Q_1))wdy}_{(**)} + \\ & \underbrace{[\delta w'h^2\beta^2 w]_0^l + [\delta w''\gamma^2 w']_0^l - [\delta w'''\gamma^2 w]_0^l}_{[k]_W^k \text{ Uncoupled}} + \underbrace{\int_0^l \delta w'(2h\beta^2)vdy}_{[k_{WV}]_{4\times2} \text{ Coupling}} \end{aligned} \tag{13}$$

Equation (12) and (13) are simply a different, yet equivalent, way of evaluating equations (4) and (5) at the element level. The follwing non-nodal approximations are defined

$$\delta v = \langle P(y) \rangle_V \{\delta a\}; \quad v = \langle P(y) \rangle_V \{a\}; \tag{14}$$

$$\delta w = \langle P(y) \rangle_W \{\delta b\}; \quad w = \langle P(y) \rangle_V \{b\}, \tag{15}$$

where $\{a\}$ and {b} are the generalized co-ordinates for v and w, respectively, with the basis functions of approximation space expressed as:

$$\langle P(y) \rangle_V = \left\langle \cos(\varepsilon y) \quad \sin(\varepsilon y)/\varepsilon \right\rangle; \tag{16}$$

$$\langle P(y) \rangle_W = \left\langle \cos(\sigma y) \quad \frac{\sin(\sigma y)}{\sigma} \quad \frac{\cosh(\tau y) - \cos(\sigma y)}{\sigma^2 + \tau^2} \quad \frac{\sinh(\tau y) - \sin(\sigma y)}{\sigma^3 + \tau^3} \right\rangle, \tag{17}$$

where ε, σ and τ (shown below) are calculated based on the characteristic equations (*) and (**) in expressions (12) and (13) being reduced to zero.

$$\varepsilon = \sqrt{\omega^2 Q_1 / \alpha^2}; \quad \sigma, \tau = \sqrt{\frac{\mathrm{h}^2\beta^2 \pm \sqrt{(\mathrm{h}^2\beta^2)^2 - 4\gamma^2(\alpha^2/R^2 - \omega^2 Q_2)}}{2\gamma^2}} \tag{18}$$

The non-nodal approximations (14) and (15) are made for δv, v, δw and w so that the integral terms (*) and (**) in expressions (12) and (13) become zero. The former term has a 2nd-order characteristic equation of the form $A_1D^2 + B_1\omega^2 = 0$, whereas the latter one has a 4th-order characteristic equation of the form $A_2D^4 - B_2D^2 + C_2\omega^2 = 0$. Solving (*) and (**) yields the solution to the uncoupled parts of (12) and (13), which are subsequently used as the dynamic basis functions of approximation space to derive the DTSFs. The nodal approximations for *element* variables, $v(y)$ and $w(y)$, are then written as:

$$v = \langle P(y) \rangle_V [\mathrm{P_n}]_\mathrm{V}^{-1} \{\mathrm{u_n}\}_\mathrm{V} = \langle N(y) \rangle_V \{v_1 \quad v_2\}; \tag{19}$$

$$w = \langle P(y) \rangle_V [\mathrm{P_n}]_\mathrm{W}^{-1} \{\mathrm{u_n}\}_\mathrm{W} = \langle N(y) \rangle_W \{w_1 \quad w'_1 \quad w_2 \quad w'_2\}; \tag{20}$$

where <$N(y)_v$> and <$N(y)_w$> are the dynamic (frequency-dependent), trigonometric, shape functions, DTSFs, of the approximation space. Similar expressions are also written for the weighting functions, $\delta v(y)$ and $\delta w(y)$. Substituting the above nodal approximations into (12) and (13) and carrying out the integrations and term evaluations leads to the following matrix form:

$$\mathrm{W}^{\mathrm{k}} = ([k]_{V\ \text{Uncoupled}}^{k} + [k]_{W\ \text{Uncoupled}}^{k} + [k]_{V\ \text{Coupling}}^{k})\{u_n\} = [k(\omega)]^{k}\{u_n\} \tag{21}$$

where $[k(\omega)]^k$ represents the frequency-dependent *element* dynamic stiffness matrix for coupled bending-axial vibrations of a curved symmetric sandwich beam element k. The appendix provides a more in-depth description of the process used to obtain the element matrices. The standard assembly method is used to obtain the global equation:

$$\mathrm{W} = \sum_{k=1}^{\text{Number of Elements}} W^k = \langle \delta U \rangle [k(\omega)]\{U\} = 0 \tag{22}$$

where $[k(\omega)]$ is the global, overall, dynamic Stiffness Matrix (DSM), and $\{U\}$ stands for the vector of global DOFs of the system.

Matlab® program was used in the calculation of the integral terms for the element dynamic stiffness matrix. It is worth noting that Matlab® performs the calculations using complex arithmetics and as a result some of the elements in the matrix $[K]^k_{Coupling}$ are complex. However, the resulting dynamic stiffness matrix $[k(\omega)]$ is real and symmetric, with the imaginary parts of each element being zero.

It should also be pointed out that in equation (12) an integral term containing "$\delta v(4\beta^2)vdy$", was purposely left out of (*). This term represents the effect of the shear from the core on the face layers (S_{CF}), and its inclusion in (*) would change the trigonometric basis functions to purely hyperbolic functions. This, in turn, makes it impossible to find the solution to the free vibration problem. However, above a given frequency, the excluded integral term can be included in the (*) term (using, e.g., an 'if' statement) without any convergence problems. For the test cases being studied here, the critical frequency is much higher than the range being studied. Therefore, the S_{CF} term is simply evaluated separately and using the originally proposed basis functions (16) and (17).

5. Numerical tests and results

The DFE is used to compute the natural frequencies and modes of curved symmetrical sandwich beams. The solution to the problem lies in finding the system eigenvalues (natural frequencies, ω), and eigenvectors (natural modes). A simple determinant search method is utilized to compute the natural frequencies of the system. The beam considered has a span of S = 0.7112 m, a radius of curvature of R = 4.225 m, with the top and bottom faces having thicknesses of t = 0.4572 mm, and a core thickness of t_c = 12.7 mm. The material properties of the face layers are: E = 68.9 GPa and ρ_f = 2680 kg/m^3, while the core has properties of G_c = 82.68 MPa and ρ_c = 32.8 kg/m^3.

5.1 Cantilever end conditions

The first test case investigates the natural frequencies of the beam described above, with cantilever end conditions. The DFE and FEM results (Table 1) are presented and compared with those reported by Ahmed (1971), obtained from a 10-element FEM model of 2-noded 8-DOFs beam elements. The model developed by Ahmed employs polynomial cubic Hermite shape functions for the approximation space of the field variables v, v', w and w'.

ω_n rad/s	FEM, 10-Elem. Ahmed, 1971	DFE 20-Elem.	DFE 30- Elem.	DFE 40-Elem.	FEM; 3-DOF/node		FEM; 4-DOF/node	
					20-Elem.	40-Elem.	20-Elem.	40-Elem.
ω_1	1124.69	1124.69	1121.93	1121.8	1121.67	1121.61	1121.61	1121.61
ω_2	1671.33	1678.87	1671.89	1668.37	1668.25	1665.67	1665.48	1664.98
ω_3	3430.62	3451.98	3420.38	3408.88	3420.32	3402.97	3402.41	3398.51
ω_4	5868.50	5901.80	5838.65	5817.10	5860.33	5811.82	5811.07	5799.69
ω_5	8664.51	8695.93	8600.30	8567.37	8659.42	8566.24	8564.74	8524.02

Table 1. Natural frequencies (rad/s) of a clamped- free curved symmetric sandwich beam

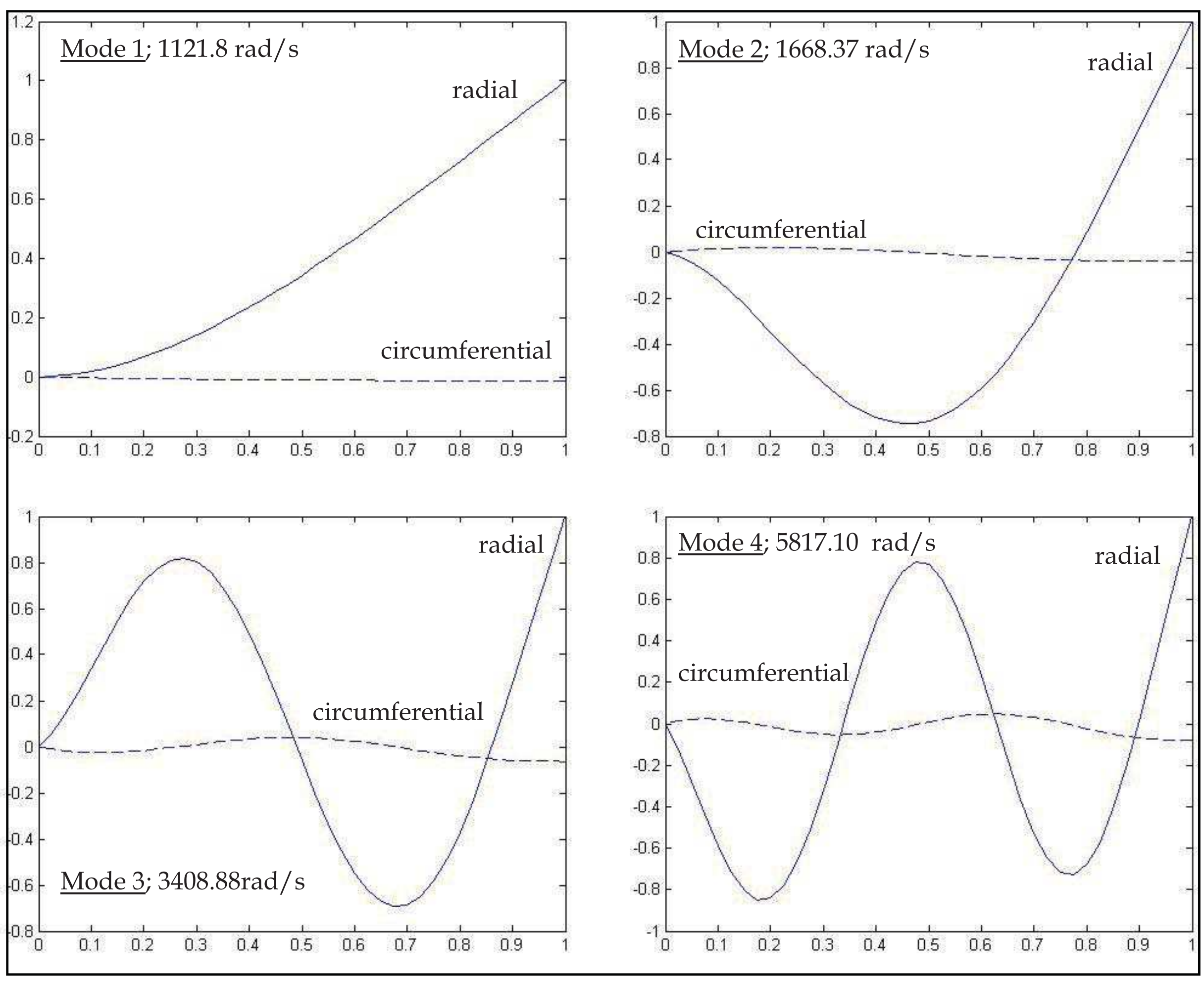

Fig. 3. First four ormalized modes for cantilever curved symmetric sandwich beam

The frequency results for the FEM and DFE models agree very well with one another with the maximum difference of 1.53% for the fifth natural frequency for 20-element models

when comparing the DFE and the 4-DOF FEM. For the 40-element models, the largest difference is 0.51% again for the fifth mode when comparing the DFE and 4-DOF FEM. Also, the first four normalized modes were computed using DFE model for the cantilevered curved sandwich beam and are shown in the Figure 3 below, generated using a 40-element DFE model. The curved beam has a large radius of curvature compared to its span, so the mode shapes of a straight beam can be used as a rough guideline to gauge the acceptability of the current modes. The frequency values used in the calculations of the mode shapes of the beam are 99.99% of the natural frequencies because the displacements cannot be evaluated as the true value of the natural frequency is approached.
As can be seen in Figures 3, all the mode shapes are dominated by radial displacements. This was expected as the bending stiffness of the beam is much smaller than its axial stiffness and the primary concern of the equations derived by Ahmed was to study the flexural behaviour of the beam (The undeformed shape of the beam was not included in the figures above because the beam's short length (0.7112) with respect to its large radius of curvature (4.225 m) would make the beam appear nearly straight).

5.2 Clamped-Clamped (C-C) end conditions

The next test case uses the same beam properties as the previous example, with clamped-clamped end conditions. The results of the DFE, and 3- and 4-DOF/node FEM formulations along with those reported by Ahmed (1971,1972) are listed in Table 2 below. For the first set of results from Ahmed (1971), shown in the second column of Table 2 below, each node has 4-DOFs. The 10-element FEM model developed employs similar polynomial Hermite shape functions such as those found in equations (10) and (11) for the approximation space of the field variables v, v', w and w', respectively. The results from Ahmed (1972), shown in the third column of Table 2, are from a 10-element FEM model where each node has 6-DOFs. The DOFs, in this case, are associated with circumferential displacement (v and v'), radial displacement (w and w') and transverse shear in the x-y plane (φ and φ', which none of the derived models takes into account). For each of the displacements, a Hermite polynomial shape function similar to expressions (10) and (11) was used to define the approximation space for both the field variables and weighting - or test - functions.

ω_n	FEM						DFE		
	10 Elements Ahmed, 1971, 1972		3-DOF		4-DOF		20 Elem.	30 Elem.	40 Elem.
	4-DOF	6-DOF	20-Elem	40-Elem	20-Elem	40-Elem			
ω_1	1658.76	1507.96	1653.73	1649.96	1649.84	1648.96	1665.67	1655.62	1652.23
ω_2	3279.82	2978.23	3272.97	3249.60	3250.92	3244.20	3295.53	3263.30	3252.30
ω_3	5585.75	5296.73	5563.57	5502.19	5508.34	5488.74	5580.10	5520.47	5499.99
ω_4	8243.54	7872.83	8208.29	8093.94	8107.70	8069.37	8203.96	8112.91	8081.62
ω_5	11102.4	10662.6	11054.8	10878.2	10900.1	10839.1	11020.1	10896.0	10853.0

Table 2. Natural frequencies (rad/s) of a clamped- clamped curved symmetric sandwich beam

Table 2 above, shows that for the first two natural frequencies, the DFE results are slightly larger than those obtained from both FEM formulations, but for the 3rd-5th frequencies, the DFE values are smaller than those found by the 3-DOF FEM formulation but larger than the

4-DOF FEM formulation. For 20-element FEM models, the largest difference is 1.4% seen between the 3-DOF and 4-DOF FEM formulations (in the 5th natural frequencies), but when the number of elements is increased to 40, the difference reduces to 0.36%, which is still the largest when comparing all three models.

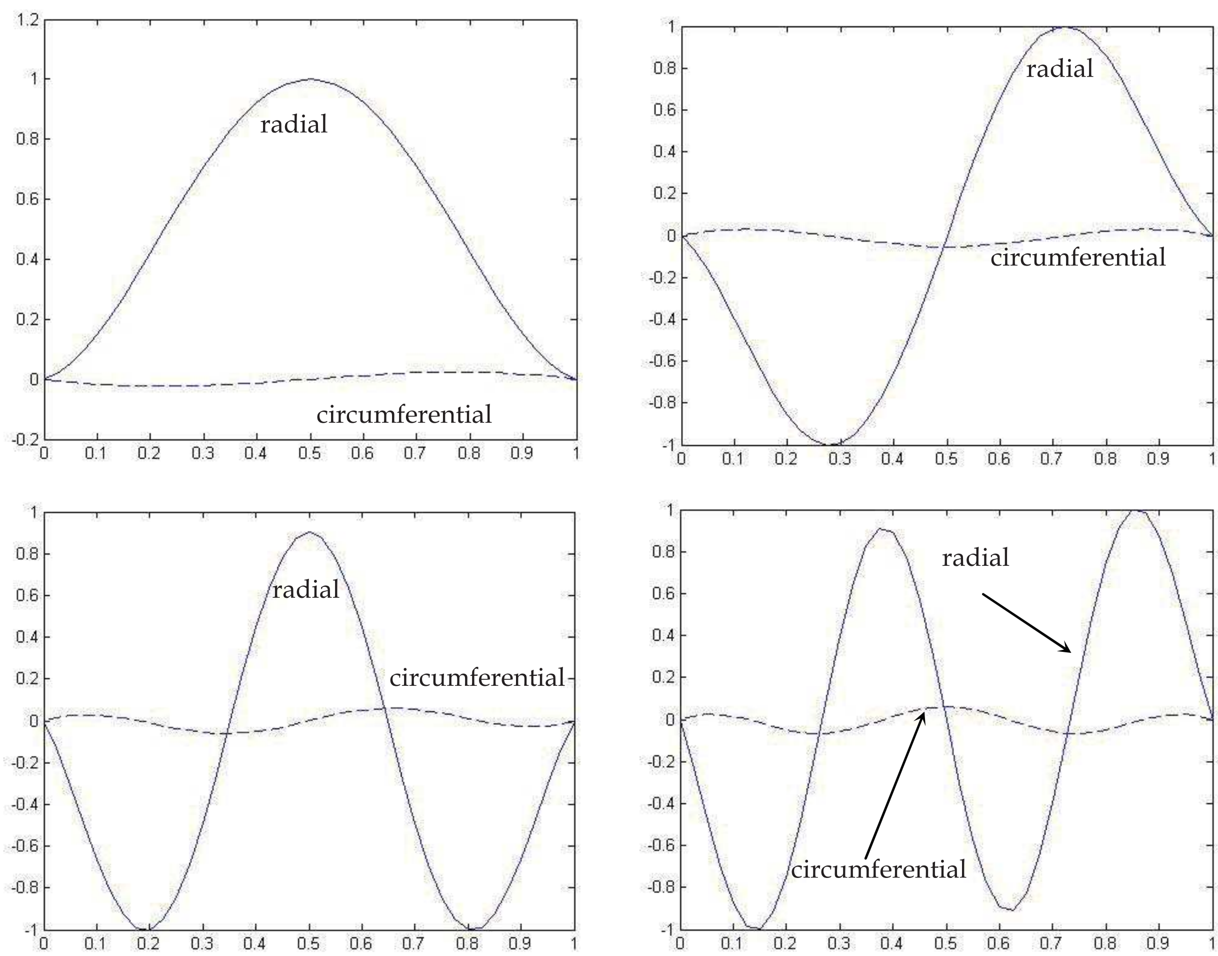

Fig. 4. First four ormalized modes for clamped-clamped curved symmetric sandwich beam

The largest difference when comparing the 40-element DFE and 3-DOF FEM models is 0.23% for the 5th natural frequency with the rest of the error being smaller. When comparing the 40-element DFE and 4-DOF FEM models, the largest error is 0.25% for the 2nd mode. The dramatic decrease in the discrepancies of the three models indicates that they are all converging to nearly the same values for the natural frequencies. When comparing the results to those of Ahmed, it can be seen that they agree very well with the 4-DOF model, although, they are smaller in value. The main reason for this is that Ahmed only used 10 elements and an increase in the number of elements used would give lower values. From Ahmed's results for the 6-DOF model, it can be seen that they are considerably lower than all the calculated values. When comparing the DFE to Ahmed's 6-DOF formulation, the largest differences can be seen for the first two natural frequencies with a difference of 9.56% and 9.20%, respectively. For the 3rd, 4th and 5th frequencies, the difference between the DFE and Ahmed 6-DOF formulation is 3.84%, 2.65% and 1.79%, respectively. Ahmed (1971) states that the difference in values is most likely due to the differences in formulations

between the two models. The equations of motion upon which the DFE is based on ignores the shear of the face layers and the bending and axial stiffness of the core while the 6-DOF formulation takes all of these factors into account.
The normalized natural modes of the curved sandwich beam, generated using a 40-element DFE model, are shown in Figures 4. As expected, the mode shapes for the curved symmetrical sandwich beam with clamped-clamped end conditions exhibit mainly radial displacement. Some circumferential displacement is also observed but is small when compared the magnitude of the radial displacement. This can be explained by the fact that the beam's axial stiffness is much higher than its bending stiffness. Also, the mode shapes conform to the clamped-clamped boundary conditions applied to the beam; the radial and circumferential displacements are zero at the end points, as is also the slope.

5.3 Simply supported-Simply supported (S-S) end conditions

The third numerical case uses the beam described earlier in the chapter with both ends simply supported. The DFE, 3- and 4-DOF FEM formulations are used to calculate the beam's natural frequencies and mode shapes. The results of these models are listed along with those reported by Ahmed (1971), obtained using a 10-element FEM model with 4-DOFs per node (see Table 3). The FEM model developed by Ahmed uses polynomial Hermite shape functions similar to equations (10) and (11) for the approximation space of the field variables v, v', w and w', respectively.
As can be seen from the 2nd row in Table 3, there is a good agreement between all the 20-element models, with the biggest discrepancy being between the DFE and the 4-DOF FEM formulations; the FEM 1st natural frequency is only 0.41% smaller than that obtained from the DFE. However, when the remaining frequencies are examined, the growing difference can be observed for the higher modes. When comparing the 20-element DFE and the 20-element 3-DOF FEM formulations, the largest difference is for the 2nd natural frequency, with the FEM value being 1.21% smaller than the DFE result. The difference between the DFE and 3-DOF FEM results decreases with increasing mode number.

ω_n	FEM					DFE		
	4DOF; 10-Elem. Ahmed, 1971	3DOF		4DOF		20-Elem.	30-Elem.	40-Elem.
		20-Elem.	40-Elem.	20-Elem.	40-Elem.			
ω_1	1253.5	1248.60	1248.34	1248.34	1248.34	1253.50	1250.35	1249.47
ω_2	2475.58	2471.74	2466.65	2464.89	2464.89	2501.96	2480.60	2472.87
ω_3	4687.26	4690.84	4669.22	4662.06	4662.06	4746.95	4697.94	4680.97
ω_4	7382.74	7405.49	7354.72	7337.82	7337.82	7478.88	7397.82	7370.11
ω_5	10298.1	10351.3	10261.4	10231.4	10231.4	10433.9	10318.9	10279.0

Table 3. Natural frequencies (rad/s) of a simply-supported curved symmetric sandwich beam

Increasing the number of elements from 20 to 40, reduces the difference between the two models for the 2nd frequency to 0.25% remaining the maximum and the difference for the other frequencies decreasing with the increase in mode number.
Comparing the 20-element DFE and the 4-DOF FEM models, the trend is reversed; the two values are closest for the 1st natural frequency and increase with the higher modes with the

largest difference being for the 5th frequency, where the FEM value is 1.94% smaller than that of the DFE. When the number of elements used in the model is increased to 40, the agreement between the two formulations becomes much better with the maximum relative error being 0.46% for the 5th frequency. Increasing the number of elements from 20 to 40 considerably reduces the relative error between all the models; i.e., convergence. For the 1st natural frequency, there is a perfect match between Ahmed's results and the 20-element DFE model. But with the increase in the mode number, the difference between the DFE and Ahmed's results grow to a maximum of 1.32% for the 5th natural frequency.

As seen in Table 3 above, increasing the number of elements in the DFE to 40 reduces the values of all the DFE frequencies lower than those reported by Ahmed; the maximum difference is now in the 1st mode, with the DFE frequency 0.32% smaller than the value reported by Ahmed. Although increasing the number of elements seems to have gone in the opposite direction of what it was intended, it should be noted that Ahmed (1971) only used 10 elements in the reported FEM results and based on the trend observed, increasing the number of elements will lower the values of the frequencies, better matching the DFE results.

Using the 40-element DFE model, the mode shapes are calculated and illustrated in Figures 5 below. The mode shapes were found using values 99.99% of the actual natural frequencies

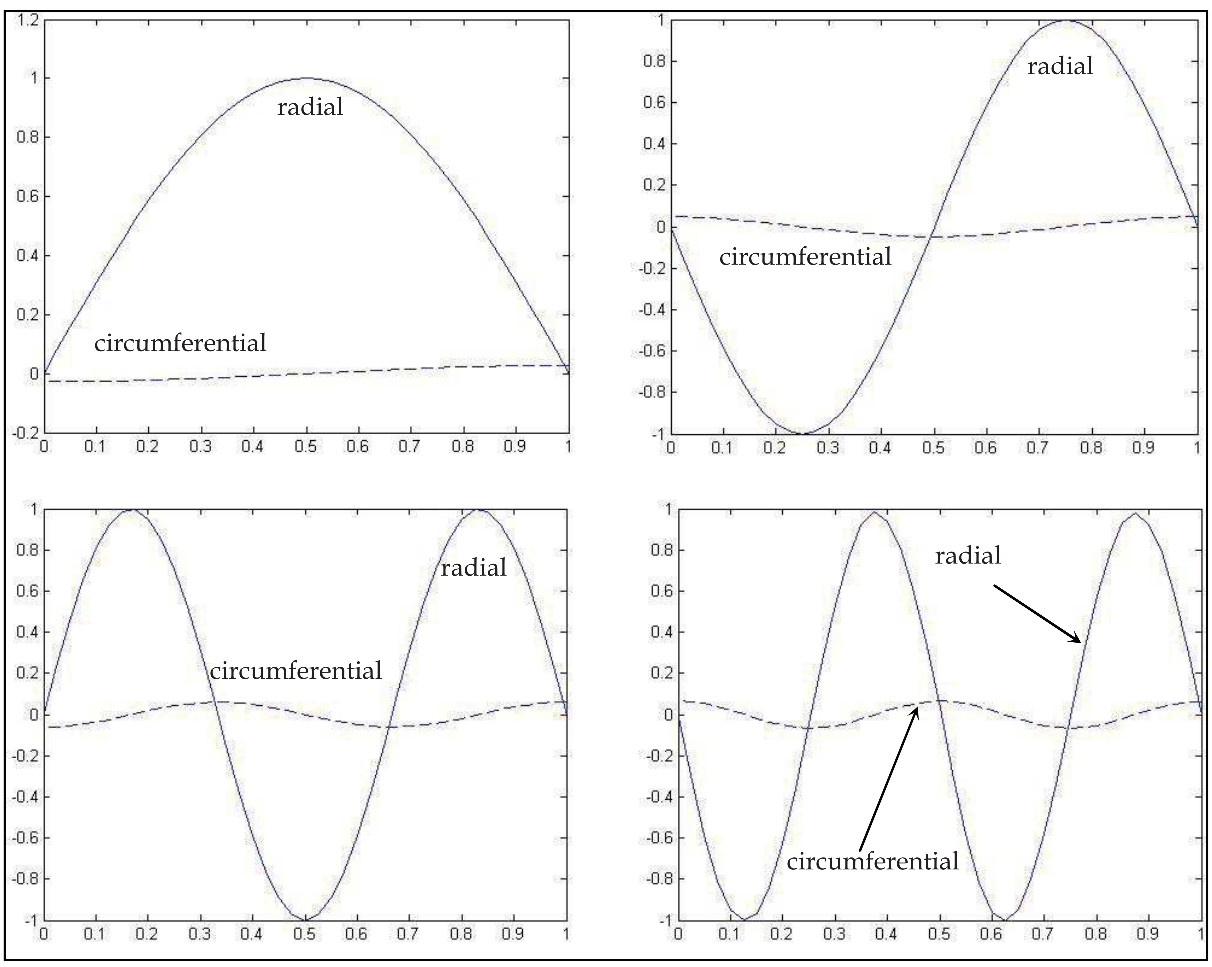

Fig. 5. First four normalized modes for clamped-clamped curved symmetric sandwich beam

of the system because displacements of the system become impossible to evaluate at the values near the natural frequencies. As can be seen from Figures 5, the mode shapes for the curved symmetric sandwich beam with simply supported end conditions are dominated by radial displacement which is the expected result due to the beam's high axial stiffness in comparison to its bending stiffness. It is worth noting that at the end points some axial displacement is observed. This is in accordance with the fact that for the simply supported end condition, the circumferential displacement is not forced to zero, giving the possibility of a non-zero value for displacement at the end points.

5.4 Simply-Supported (S-S) straight symmetric sandwich beam

In the final numerical test, the curved symmetrical sandwich beam formulation is applied to a straight beam case. The beam has a length of S = 0.9144 m, radius $R = \infty$, with face thickness t = 0.4572 mm and core thickness t_c = 12.7 mm. The mechanical properties of the face layers are: E = 68.9 GPa and ρ_f = 2680 kg/m^3, while the core has properties of G_c = 82.68 MPa and ρ_c = 32.8 kg/m^3. The natural frequencies of the beam are calculated using the DFE method as well as the 3-DOF and 4-DOF FEM formulations and compared to the data published by Ahmed (1971) (see Table 4). In the case of a straight beam, the radial displacement and circumferential displacements directly translate into the flexural and axial displacements, respectively.

ω_n	FEM					DFE		
	Ahmed,1971 4DOF 10-Elem	3DOF		4DOF		20-Elem.	30-Elem.	40-Elem.
		20-Elem.	40-Elem.	20-Elem	40-Elem.			
ω_1	361.35	359.27	359.02	358.90	358.90	370.02	363.55	361.41
ω_3	2938.6	2940.5	2924.3	2918.9	2918.9	3012.4	2958.6	2952.72
ω_5	6980.6	7044.7	6966.0	6939.9	6939.8	7169.2	6993.5	6987.1
ω_7	11574.	11740.	11559.	11498.	11498.	11885.	11667	11591.
ω_9	16299.	16582.	16284.	16184.	16182.	16729.	16423.	16316.

Table 4. Natural frequencies (rad/s) of a simply-supported straight symmetric sandwich beam

6. Conclusion

Based on the theory developed by Ahmed (1971,1972) and the weak integral form of the differential equations of motion, a dynamic finite element (DFE) formulation for the free vibration analysis of symmetric curved sandwich beams has been developed. The DFE formulation models the face layer as Euler-Bernoulli beams and allows the core to deform in shear only. The DFE formulation is used to calculate the natural frequencies and mode shapes for four separate test cases. In the first three cases the same curved beam, with different end conditions, are used: cantilever, both ends clamped and lastly, both ends simply supported. The final test case used the DFE formulation to determine the natural frequencies of a simply supported straight sandwich beam.

All the numerical tests show satisfactory agreement between the results for the developed DFE, FEM and those published in literature. For all test studies, when a similar number of elements are used, the DFE matched more closely with the 3-DOF FEM formulation than with Ahmed's 4-DOF FEM results. The reason for this is that the DFE is derived from the 3-

DOF FEM formulation and such a trend is expected. Ahmed (1971) goes on to explain that the addition of an extra degree of freedom for each node has a tendency to lower the overall stiffness of a sandwich beam element causing an overall reduction in values of the natural frequencies. The mode shapes determined by the DFE formulation match the expectations based on previous knowledge on the behaviour of straight sandwich beams. The results of the DFE theory and methodology applied to the analysis of a curved symmetric sandwich beam demonstrate that DFE can be successfully extended from a straight beam case to produce a more general formulation. The proposed DFE is equally applicable to the piecewise uniform (i.e., stepped) configurations and beam-structures. It is also possible to further extend the DFE formulation to more complex configurations and to model geometric non-uniformity and material changes over the length of the beam.

7. Acknowledgement

The support provided by Natural Science and Engineering Research Council of Canada (NSERC), Ontario Graduate Scholarship (OGS) Program, and High Performance Computing Virtual Laboratory (HPCVL)/Sun Microsystems is also gratefully acknowledged.

8. Appendix: development of DFE Stiffness matrices for curved symmetric Euler-Bernoulli/Shear sandwich beam

The Dynamic Finite Element stiffness matrix for a symmetric curved sandwich beam is developed from equations (12) and (13) found in Section 4. Applying the approximations for the element variables, $v(y)$ and $w(y)$, and the test functions, $\delta v(y)$ and $\delta w(y)$, as shown in expressions (19) and (20) to *element* integral equations (12) and (13) yield the *element* DFE stiffness matrix defined in equation (21).
First, let us consider the *element* virtual work corresponding to the circumferential displacement, $v(y)$. Based on the governing differential equation (1), the critical value, or *changeover frequency*, is then determined from

$$\omega^2 Q_1 - 4\beta^2 = 0 \tag{A1}$$

For the frequencies below the *changeover frequency*, the element integral equation (12) can be expressed as:

$$W_V^k = \underbrace{-\int_0^l (\delta v''\alpha^2 + \delta v\omega^2 Q_1)v dy}_{(*)} + \underbrace{\int_0^l \delta v(4\beta^2)v dy + [\delta v'\alpha^2 v]_0^l}_{[k]_V^k \text{ Uncoupled}} + \underbrace{\int_0^l (\delta v 2h\beta^2)w' dy}_{[k_{VW}]_{2\times4} \text{ Coupling}} \quad \text{(12 repeated)}$$

where the first integral term, (*) vanishes due to the choice of the trigonometric basis function for $v(y)$, as stated in:

$$< P(y) >_V = \langle \cos(\varepsilon y) \;\; \sin(\varepsilon y)/\varepsilon \rangle; \quad \text{(16 repeated)}$$

The next two terms, produce a symmetric 2x2 matrix $[\ k\ ]_V^k$ that contains all the uncoupled stiffness matrix elements associated with the displacement $v(y)$. The inclusion of S_{CF} term in

(*) would make the solution to the corresponding characteristic equation (also used as basis functions of approximation space) change form trigonometric to purely hyperbolic functions. This, in turn, would lead to solution divergence of the DFE formulation, where natural frequencies of the system cannot be reached using the determinant search method.
For the test cases examined here, the *changeover frequency* for the faces is well above the range of frequencies being studied; therefore, the S_{CF} term, representing the shear effect from the core on the face layers, is kept out of the integral term (*) and evaluated as a part of the second term, $[\,k\,]_V^k$.
For the frequencies above the *changeover frequency*, the element integral equation can be re-written as:

$$W_V^k = -\underbrace{\int_0^l (\delta v''\alpha^2 + \delta v(\omega^2 Q_1 - 4\beta^2)v dy}_{(*)} + \underbrace{[\delta v'\alpha^2 v]_0^l}_{[k]_V^k \text{ Uncoupled}} + \underbrace{\int_0^l (\delta v 2h\beta^2) w' dy}_{[k_{VW}]_{2\times4} \text{ Coupling}} \tag{A2}$$

where the S_{CF} term is included in the integral term (*), which vanishes due to the choice of purely trigonometric basis functions for *v(y)*, similar to (16). The next term, then produces a symmetric 2x2 matrix $[\,k\,]_V^k$ that contains all the uncoupled stiffness matrix elements associated with the displacement *v(y)* and the final term, produces a 2x4 matrix $[k_{VW}]$ that contain all the terms that couple the displacement *v(y)* with *w(y)*.

$$[k]_V^k = \begin{bmatrix} k_V(1,1) & k_V(1,2) \\ sym. & k_V(2,2) \end{bmatrix} \tag{A3}$$

$$[k_{VW}]^k = \begin{bmatrix} k_{VW}(1,1) & k_{VW}(1,2) & k_{VW}(1,3) & k_{VW}(1,4) \\ k_{VW}(2,1) & k_{VW}(2,2) & k_{VW}(2,3) & k_{VW}(2,4) \end{bmatrix} \tag{A4}$$

Now considering equations (13):

$$W_W^k = \underbrace{\int_0^l (\delta w''''\gamma^2 - \delta w'' h^2\beta^2 + \delta w(\alpha^2/R^2 - \omega^2 Q_1))w dy}_{(**)} + \\ \underbrace{[\delta w' h^2\beta^2 w]_0^l + [\delta w''\gamma^2 w']_0^l - [\delta w'''\gamma^2 w]_0^l}_{[k]_W^k \text{ Uncoupled}} + \underbrace{\int_0^l \delta w'(2h\beta^2) v dy}_{[k_{WV}]_{4\times2} \text{ Coupling}} \tag{13 repeated}$$

The first integral term, (**), in equation (13), vanishes due to the choice of mixed trigonometric-hyperbolic basis functions for *w(y)*, similar to (17):

$$< P(y) >_W = \left\langle \cos(\sigma y) \quad \frac{\sin(\sigma y)}{\sigma} \quad \frac{\cosh(\tau y) - \cos(\sigma y)}{\sigma^2 + \tau^2} \quad \frac{\sinh(\tau y) - \sin(\sigma y)}{\sigma^3 + \tau^3} \right\rangle, \tag{17 repeated}$$

The next three terms, produce a symmetric 4x4 matrix $[k]_W^k$ that contain all the uncoupled stiffness matrix elements associated with the displacement *w(y)*. The final term, produces a 4x2 matrix $[k_{WV}]$ that contain all the terms that couple the displacement *w(y)* with *v(y)*. It is important to note that $[k_{WV}] = [k_{VW}]^T$.

$$[k]_W^k = \begin{bmatrix} k_W(1,1) & k_W(1,2) & k_W(1,3) & k_W(1,4) \\ & k_W(2,2) & k_W(2,3) & k_W(2,4) \\ & & k_W(3,3) & k_W(3,4) \\ sym. & & & k_W(4,4) \end{bmatrix} \tag{A5}$$

$$[k_{WV}]^k = \begin{bmatrix} k_{WV}(1,1) & k_{WV}(1,2) \\ k_{WV}(2,1) & k_{WV}(2,2) \\ k_{WV}(3,1) & k_{WV}(3,2) \\ k_{WV}(4,1) & k_{WV}(4,2) \end{bmatrix} \tag{A6}$$

Matrices (A3), (A4), (A5) and (A6) are added according to equation (21) in order to obtain the 6x6 element stiffness matrix for a symmetric straight sandwich beam.

$$[k]^k = \begin{bmatrix} k_V(1,1) & k_{VW}(1,1) & k_{VW}(1,2) & k_V(1,2) & k_{VW}(1,3) & k_{VW}(1,4) \\ & k_W(1,1) & k_W(1,2) & k_{WV}(1,2) & k_W(1,3) & k_W(1,4) \\ & & k_W(2,2) & k_{WV}(2,2) & k_W(2,3) & k_W(2,4) \\ & & & k_V(2,2) & k_W(2,3) & k_W(2,4) \\ & & & & k_W(3,3) & k_W(3,4) \\ sym. & & & & & k_W(4,4) \end{bmatrix} \tag{A7}$$

9. References

Adique E. & Hashemi S.M. (2007). Free Vibration of Sandwich Beams using the Dynamic Finite Element Method", in B.H.V. Topping, (Editor), "Proceedings of the Eleventh International Conference on Civil, Structural and Environmental Engineering Computing", Civil-Comp Press, Stirlingshire, UK, Paper 118, 2007. doi:10.4203/ccp.86.118, St. Julians, Malta. 18-21 Sept 2007.

Adique E. & Hashemi S.M. (2008). Dynamic Finite Element Formulation and Free Vibration Analysis of a Three-layered Sandwich Beam," Proceedings of The 7th Joint Canada-Japan Workshop on Composite Materials, July 28-31, 2008, Fujisawa, Kanagawa, Japan, pp. 93-100.

Adique E. & Hashemi S.M. (2009). A Super-Convergent Formulation for Dynamic Analysis of Soft-Core Sandwich Beams", in B.H.V. Topping, L.F. Costa Neves, R.C. Barros, (Editors), "Proceedings of the 12th International Conference on Civil, Structural and Environmental Engineering Computing", Civil-Comp Press, Stirlingshire, UK, Paper 98, 2009. doi:10.4203/ccp.91.98, Funchal, Madeira Island, 1-4 Sept. 2009.

Ahmed, K. M. (1971). Free vibration of curved sandwich beams by the method of finite elements. *Journal of Sound and Vibration,* Vol. 18, No. 1, (September 1971) 61-74, ISSN: 0022-460X.

Ahmed, K. M. (1972). Dynamic analysis of sandwich beams. *Journal of Sound and Vibration,* Vol. 21, No. 3, (April 1972) 263-276, ISSN: 0022-460X.

Baber, T.T.; Maddox, R.A. & Orozco, C.E. (1998). A finite element model for harmonically excited viscoelastic sandwich beams. *Computers &Structures,* Vol. 66, No. 1, (January 1998) 105-113, ISSN: 0045-7949.

Banerjee, J. R. (1999). Explicit frequency equation and mode shapes of a cantilever beam coupled in bending and torsion. *Journal of Sound and Vibration*, Vol. 224, No. 2, (July 1999) 267-281, ISSN: 0022-460X.

Banerjee, J. R. (2001). Explicit analytical expressions for frequency equation and mode shapes of composite beams. *International Journal of Solids and Structures*, Vol. 38, No. 14 (April 2001) 2415-2426, ISSN: 0045-7949.

Banerjee, J. R. (2001). Frequency equation and mode shape formulae for composite Timoshenko beams. *Composite Structures,* Vol. 51, No. 4, (May 2001) 381-388, ISSN: 0045-7949.

Banerjee, J. R. (2001). Dynamic stiffness formulation and free vibration analysis of centrifugally stiffened Timoshenko beams. *Journal of Sound and Vibration* , Vol. 247, No. 1, (October 2001) 97-115, ISSN: 0022-460X.

Banerjee, J. R. (2003). Free vibration of sandwich using the dynamic stiffness method. *Computers &Structures*, Vol. 81, No. 18-19 (August 2003) 1915-1922, ISSN: 0045-7949.

Banerjee, J. R.; Cheung, C. W.; Morishima, R.; Perera, M. & Njuguna, J. (2007). Free vibration of a three-layered sandwich beam using the dynamic stiffness method and experiment. *International Journal of Solids and Structures*, Vol. 44, No. 22-23 (November 2007) 7543-7563, ISSN: 0045-7949.

Banerjee, J. R. and Sobey, A. J. (2005). Dynamic stiffness formulation and free vibration analysis of a three-layered sandwich beam. *International Journal of Solids and Structures,* Vol. 42, No. 8, (2005) 2181-2197, ISSN: 0045-7949.

Banerjee, J. R. And Su, H. (2004). Development of a dynamic stiffness matrix for free vibration analysis of spinning beams. *Computers &Structures*, Vol. 82, No. 23-24 (September - October 2004) 2189-2197, ISSN: 0045-7949.

Banerjee, J. R. and Su, H. (2006). Dynamic stiffness formulation and free vibration analysis of a spinning composite beam. *Computers &Structures*, Vol. 84, No. 19-20, (July 2006) 1208-1214, ISSN: 0045-7949.

Banerjee, J. R. & Williams, F.W. (1996). Exact dynamic stiffness matrix for composite Timoshenko beams with applications. *Journal of Sound and Vibration*, Vol. 194, No. 4, (July 1996), 573-585, ISSN: 0022-460X.

Banerjee, J. R. & Williams, F.W. (1995). Free vibration of composite beams – an exact method using symbolic computation. *Journal of Aircraft* , Vol. 32, No. 3, (1995) 636-642, ISSN: 0021-8669.

Di Taranto, R. A. (1965). Theory of vibratory bending for elastic and viscoelastic layered finite length beams. *Journal of Applied Mechanics*, Vol. 87, (1965) 881-886, ISSN: 0021-8936 (Print), eISSN: 1528-9036.

Fasana, A. & Marchesiello, S. (2001). Rayleigh-Ritz analysis of sandwich beams. *Journal of Sound and Vibration*, Vol. 241, No. 4, 643-652, ISSN: 0022-460X.

Hashemi, S. M. (1998). *Free Vibration Analysis Of Rotating Beam-Like Structures: A Dynamic Finite Element Approach*. Ph.D. Dissertation, Department of Mechanical Engineering, Laval University, Québec, Canada.

Hashemi, S. M. (2002). The use of frequency dependent trigonometric shape functions in vibration analysis of beam structures – bridging the gap between FEM and exact DSM formulations. *Asian Journal of Civil Engineering*, Vol. 3, No. 3&4, (2002) 33-56, ISSN: 15630854.

Hashemi, S. M. & Adique, E.J. (2009). Free Vibration analysis of Sandwich Beams: A Dynamic Finite Element, *International Journal of Vehicle Structures & Systems (IJVSS),* Vol. 1, No 4, (November 2009) 59-65, ISSN: 0975-3060 (Print), 0975-3540 (Online).

Hashemi, S. M. & Adique, E.J (2010). A Quasi-Exact Dynamic Finite Element for Free Vibration Analysis of Sandwich Beams, *Applied Composite Materials,* Vol. 17, No. 2, (April 2010) 259-269, ISSN: 0929-189X (print version, 1573-4897 (electronic version), doi:10.1007/s10443-009-9109-3.

Hashemi, S. M. & Borneman, S. R. (2004). Vibration analysis of composite wings undergoing material and geometric couplings: a dynamic finite element formulation. *CD Proceedings of the 2004 ASME International Mechanical Engineering Congress (IMECE 2004,) Aerospace Division,* pp 1-7, November 2004, Anaheim, CA, USA.

Hashemi, S. M. and Borneman, S. R. (2005). A dynamic finite element formulation for the vibration analysis of laminated tapered composite beams. *CD Proceedings of the Sixth Canadian-International Composites Conference (CanCom),* pp. 1-13, August 2005, Vancouver, BC, Canada.

Hashemi, S. M.; Borneman, S. R. & Alighanbari, H. (2008). Vibration analysis of cracked composite beams: a dynamic finite element. *International Review of Aerospace Engineering (I.RE.AS.E.),* Vol. 1, No. 1, (February 2008) 110-121, ISSN: 1973-7459.

Hashemi, S. M.; Richard, M. J. & Dhatt, G. (1999). A new dynamic finite elements (DFE) formulation for lateral free vibrations of Euler-Bernoulli spinning beams using trigonometric shape functions. *Journal of Sound and Vibration,* Vol. 220, No. 4, (March 1999) 601-624, ISSN: 0022-460X.

Hashemi, S. M. & Richard, M. J. (2000a). Free vibration analysis of axially loaded bending-torsion coupled beams – a dynamic finite element (DFE). *Computers and Structures* , Vol. 77, No. 6, (August 2000) 711-724, ISSN: 0045-7949.

Hashemi, S. M. & Richard, M. J. (2000b). A dynamic finite element (DFE) for free vibrations of bending-torsion coupled beams. *Aerospace Science and Technology* , Vol. 4, No. 1, (January 2000) 41-55, ISSN: 1270-9638.

Hashemi, S. M. & Roach, A. (2008a). A dynamic finite element for coupled extensional-torsional vibrations of uniform composite thin-walled beams. *International Review of Aerospace Engineering (I.RE.AS.E.)* , Vol. 1, No. 2, (April 2008) 234-245, ISSN: 1973-7459.

Hashemi, S.M. & Roach, A. (2008b). Free vibration of helical springs using a dynamic finite element mesh reduction technique. *International Review of Mechanical Engineering*, Vol. 2, No. 3, (May 2008) 435-449 , ISSN: 1970 - 8734.

Howson, W. P. & Zare, A. (2005). Exact dynamic stiffness matrix for flexural vibration of three-layered sandwich beams. *Journal of Sound and Vibration*, Vol. 282, No. 3-5, (April 2005) 753-767, ISSN: 0022-460X.

Mead, D. J. and Markus, S. (1968). The forced vibration of a three-layer, damped sandwich beam with arbitrary boundary conditions. *Journal of Sound and Vibration,* Vol. 10, No. 2, (September 1968) 163-175, ISSN: 0022-460X.

Sainsbury, M. G. & Zhang, Q. J. (1999). The Galerkin element method applied to the vibration of damped sandwich beams. *Computers and Structures* , Vol. 71, No. 3, (May 1999) 239-256, ISSN: 0045-7949.

Wittrick, W. H. & Williams, F. W. (1971). A general algorithm for computing natural frequencies of elastic structures. *Quarterly Journal of Mechanics and Applied Mathematics,* Vol. 24, No. 3, (August 1971) 263-284, Online ISSN 1464-3855 - Print ISSN 0033-5614.

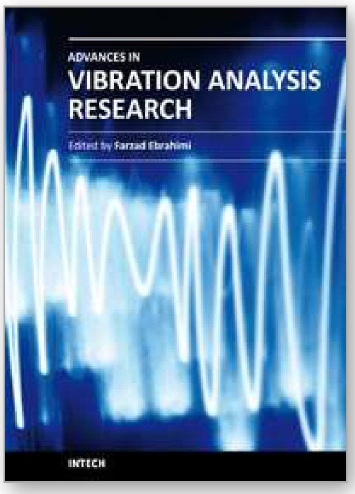

Advances in Vibration Analysis Research

Edited by Dr. Farzad Ebrahimi

ISBN 978-953-307-209-8
Hard cover, 456 pages
Publisher InTech
Published online 04, April, 2011
Published in print edition April, 2011

Vibrations are extremely important in all areas of human activities, for all sciences, technologies and industrial applications. Sometimes these Vibrations are useful but other times they are undesirable. In any case, understanding and analysis of vibrations are crucial. This book reports on the state of the art research and development findings on this very broad matter through 22 original and innovative research studies exhibiting various investigation directions. The present book is a result of contributions of experts from international scientific community working in different aspects of vibration analysis. The text is addressed not only to researchers, but also to professional engineers, students and other experts in a variety of disciplines, both academic and industrial seeking to gain a better understanding of what has been done in the field recently, and what kind of open problems are in this area.